International Journal of Fluid Power 2 (2001) No. 2 pp. 65-74

CONTROLLED VALVE PLATE IN BENT AXIS HYDRAULIC MOTORS

Alex V. Khrapak

Odessa State Academy of Refrigeration, Dvoryanskaya 1/3, 65026 Odessa, Ukraine
alexand@eurocom.od.ua

Abstract

The research object of the given work is the bent axis hydraulic motor (BAHM). In this paper the interaction of the rotating cylinder block and motionless valve plate (VP) is investigated. The research aims are focused on evaluation of the experimental and theoretical data of the VP friction torque and hydraulic fluid leakages. The up-to-date technologies require the BAHM components to be more reliable and durable. On the way of BAHM design improvement, the new VP is introduced in this paper. The new design features provide more reliable fluid lubrication in the gap between VP and cylinder block and increase the durability of the piston cylinder assembly in heavy operation modes. The laboratory tests proved the efficiency of the new VP design.

Keywords: bent axis hydraulic motor, valve plate, hydraulic fluid, fluid leakage

1 Introduction

As a rule, the VP provides the fluid distribution in BAHM operation modes. The VP may be designed as a separate unit, or as a disk and a back cover assembly. The front face of the VP has two kidney ports which are separated by the sealing walls (Khrapak, 2000). The VP principle of operation in up-to-date BAHM is still the same as in 1903 – the time when BAHM was created (Bashta, 1974). In spite of the fact that there are a lot of patents and "know-how", the principle of operation of the VP is still primitive. That is why, in our days the VP is the main errorprone element of the BAHM.

The VP predetermines the high sensitivity of the BAHM to hydraulic fluids contaminations and size and contributes in establishing an adequate lubrication in the gap that exists with the barrel.

Each of the cited aspects has its own influence on durability and reliability of the motor unit.

The up-to-date tendencies of working pressure increase, require VP design improvements, because the traditional VP design (see Fig.1) doesn't provide the necessary reliability and durability of the BAHM. Also, it is necessary to take into account that VP stipulate the noise characteristics of the BAHM.

All the questions mentioned above confirm the expediency of research in this field.

This manuscript was received on 25 September 2000 and was accepted after revision for publication on 29 June 2001

2 Valve Plate influence on BAHM volumetric efficiency

The criteria for BAHM normal work are the following: thin-film lubrication in the gap between motionless valve plate (VP) and rotating cylinder block; minimal hydraulic fluid leakages.

The current task is to define the volumetric losses in the gap between cylinder block and VP, when the BAHM is operated.

The experimental investigations were made on a standard BAHM. The hydraulic fluid leakages were measured with volumetric flow sensor, the temperature with thermocouples and pressure with the pressure sensor and manometer.

Fig. 1: *Standard valve plate design*

Figure 2 shows the simplified model of the BAHM. The arrows mark the possible ways of the hydraulic fluid escape, when the BAHM is operated.

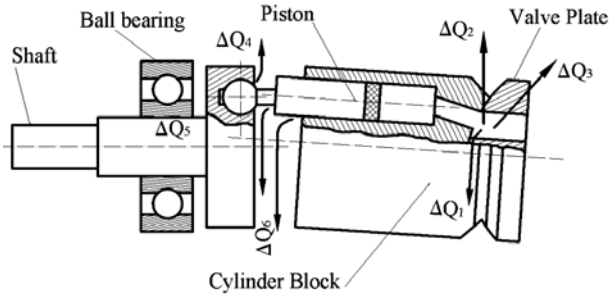

Fig. 2: *The simplified model of the bent axis hydraulic motor (BAHM)*

where: $\Delta Q_{1...3}$ – VP gap leakages;
$\Delta Q_{4...5}$ – leakages in rod and piston, rod and plate ball joints;
ΔQ_6 – leakages in piston and cylinder block gap

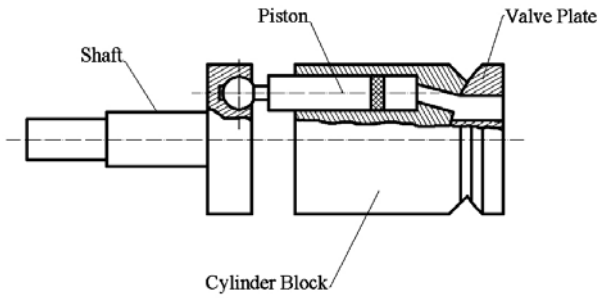

Fig. 2A: *BAHM in the test position (simplified model)*

All experiments were carried out at zero angle between the cylinder block axis and main shaft axis of the BAHM (see Fig. 2A). Flow to motor inlet was provided by displacement pump. The outlet of the pump was connected to the inlet of the BAHM. The hydraulic motor main shaft rotation was provided by the electric motor.

In the first test series the total amount of external leakages was measured. For this purpose the small collecting pan was put under the BAHM drain hole. The thermocouples were installed inside the BAHM

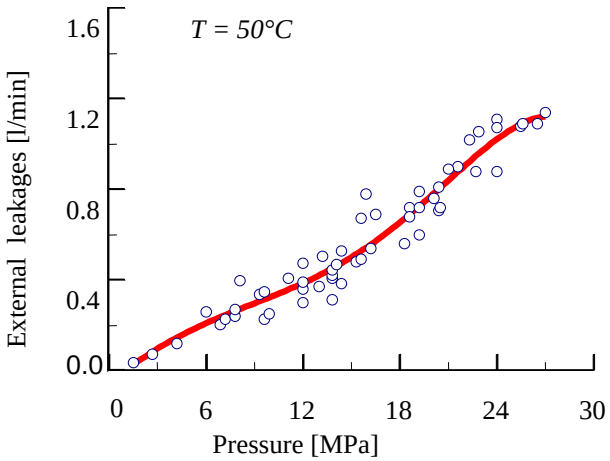

Fig. 3: *External leakages in the tested BAHM (experimental data). Hydraulic fluid temperature 50°C, shaft speed 5000 min^{-1}.*

body, near the drain hole. Measurements were carried out for the different operating parameters, such as shaft speed and inlet pressure. Figure 3 shows the dependence of all external leakages on hydraulic fluid pressure.

The analytical definition of the external leakages is complicated by many factors, which should be taken into account, here are some of them: technology details, excessive wear, deformation factor, hydraulic fluid contamination and so on.

The volumetric efficiency of the BAHM should consider all the leakages, which are shown in Fig. 1:

$$\eta_V = \frac{Q_T}{Q_{sum}} \tag{1}$$

where:

$$Q_{sum} = Q_T - (\Delta Q_1 + \Delta Q_2) - \\ - \Delta Q_{4,5} - \Delta Q_6 - \Delta Q_3$$

$Q_T = q \cdot \omega$ – BAHM ideal flow rate;
q – BAHM displacement;

The same measurement equipment and BAHM position (see Fig. 2A) was used for VP gap leakages investigation.

In this test, it was necessary to except all other leakages (such as ΔQ_4, ΔQ_5, ΔQ_6,), besides VP gap leakages (ΔQ_1, ΔQ_2, ΔQ_3). For this purpose, the gap in piston-cylinder assembly was sealed (in this test the BAHM position disables pistons movement while cylinder block rotation), so there was no way for fluid escape, besides VP gap leaks.

The hydraulic fluid leakages in the VP gap may be divided into two types: radial leakages through the sealing walls and cross port leakages.

The hydraulic fluid radial leakages are caused by radial gradients of pressure in the sealing walls and cross-port leakages by the pressure difference in the fluid layer in the gap.

The cross-port leakages from high to low pressure port can also be divided into two types. One of them has a similar basis as the outflows, it is determined by pressure gradients on sealing wall between pressure ports of the VP. These overflows depend on hydraulic fluid viscosity, VP gap height, on overlapping, and on working pressure. The other overflow type depends on: hydraulic fluid compressibility, cylinder chambers "dead" volume, and cylinder block rotational speed. This type is called fluid transfer.

Experimentally only the total value of the VP gap leakages can be measured. Figure 4 shows the dependence of the VP gap leakages on the cylinder block shaft speed.

In all experiments, the approximate amount of the radial leakages in the gap between VP and cylinder block was equal to some drops per minute ($20 \cdot 10^{-6}$...$100 \cdot 10^{-6}$). This leads us to the conclusion that the radial leakages in VP are negligible (in comparison with the all external leakages) and do not have a serious influence on BAHM volumetric performance. The quantitative estimation of the VP leakages is important, because it allows to judge work conditions of the VP.

The radial leakages depend on the cylinder block and VP gap if we assume that the gap height remains constant (Minchevich, 1983):

$$h = \sqrt{\frac{6\Delta Q_1 \mu \ln(R_2/R_1)}{\pi p_0}} \qquad (2)$$

Equation 2 shows, that the gap height is comparable with the surface microroughness of the cylinder block in high clearance class – 10…12 μm.

As it was mentioned above, the fluid film between VP and cylinder block is one of the most important conditions for the VP normal work. The hydraulic fluid radial leakages were measured and analyzed. The results brought us to the conclusion that VP works in a "heavy duty mode". The outflows are insufficient for cylinder block and VP surfaces cooling, so the VP operating conditions are close to the fluid film destruction, and there may occur the transition from the fluid friction phase to the dry friction.

Thus, the minimum of hydraulic fluid outflows – is the necessary condition for VP normal work. The important role in fluid film breakdown may be played by cylinder block surface peripheral velocity in relation to VP. The fluid layer is negligible, but it is capable to exist a very long period of time (Paulis, 1991).

The fluid film breakdown may be caused by the following factors:

- the hydraulic fluid film is transferred by the rotating cylinder block surface (inlet conditions do not restore the fluid film)
- local temperature increase due to insufficient heat transfer from the gap to the environment.

It is known, that the fluid compressibility is characterized by fluid bulk modulus, which is equal to:

$$E_V = \frac{V}{\Delta V} \cdot \Delta p \qquad (3)$$

where:

EV – fluid bulk modulus ($1.3 – 1.75 \cdot 10^9$ N/m^2)
V – total dead zone capacity ($V = V_1 \cdot z$)
V_1 – chamber dead volume;
z – number of pistons;
ΔV – fluid volume difference at Δp;
Δp – fluid pressure difference.
At motor outlet pressure may be considered as equal to zero $\Delta p = p_0$.

Obviously, the fluid volume growth ΔV is compensated by fluid transfer when the pressure in chambers is varied from p_0 to zero due to the cylinder block port crossing the separating wall:

$$\Delta V = \frac{\Delta Q_{3(\text{transfer})}}{\omega} \qquad (4)$$

Thus, the fluid transfer through the sealing walls due to the fluid compressibility, is equal to:

$$\Delta Q_{3(\text{transfer})} = \frac{V_1 \cdot z \cdot \omega \cdot p_0}{E_V} \qquad (5)$$

In this case, it is possible to neglect the cross-port leakages, which are caused by different pressures on the VP sealing walls. It is sufficiently accurate to state that the sealing wall is the main way for cross-port fluid transfer.

There are two sealing walls in the VP between input and output ports. The cylinder block peripheral velocity vector coincides with the first sealing wall pressure gradient (i.e., with leakage direction) and on the other sealing wall it has an opposite sense. This fact causes the compensation of the cylinder block distributive surface peripheral velocity influence on the separating wall cross leakages.

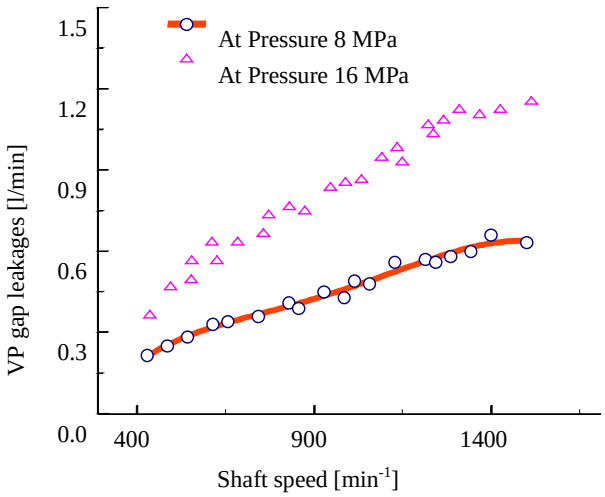

Fig. 4: *The experimental data of the VP leakages and fluid transfer*

The experimental (see Fig. 4) and the calculated data (Eq. 5) of the VP gap leakages and fluid transfer on the sealing walls are coincident, the deviation does not exceed 10 %.

Thus, cross-port fluid transfer is directly proportional to the cylinder block rotational speed and is in inverse proportion to bulk modulus.

3 VP influence on BAHM mechanical efficiency

The friction torque measurements in the BAHM (Irshov, 1993), with various grades of hydraulic fluids confirm the validity of the following equation (Murashko, 1999):

$$M_{VF} = \frac{\pi}{2} \mu e^{\alpha \cdot p} \frac{\omega}{h} \cdot \left(R_4^4 - R_1^4\right) \qquad (6)$$

where:

ω – shaft speed;
h – VP gap height;
μ – fluid dynamic viscosity;
α – pressure coefficient of viscosity;
p – working pressure;
R_4, R_1 – radii of the appropriate peripheral and inner edges of the outer and inner sealing walls of the VP.

After the improvement application, the peripheral edge radius was changed to R_6 .

For the VP friction torque measurement was used the same BAHM position as in previous experiments (see Fig. 2A). The torque from electric motor applied to BAHM main shaft was shared by VP friction and ball bearing friction, due to the pistons motionless. The measurements were carried out for different inlet pressure. The shaft speed was recorder by remote photo tachometer. Torque was measured with force transducer.

At the stable BAHM shaft rotational speed (in this case at 1000 min^{-1}), the friction torque in the ball bearing is equal to:

$$M_{BF} = f \cdot p \cdot \frac{z\pi d_p^2 d_{bt}}{16} \qquad (7)$$

Equations 6 and 7 provide us with the theoretical friction torque, and allow to obtain a theoretical curve of the friction torque (which is designated as a broken curve in Fig. 5) and compare it with the curve based on experimental data in dependence on fluid pressure.

$$M_{TF} = M_{VF} + M_{BF} \qquad (8)$$

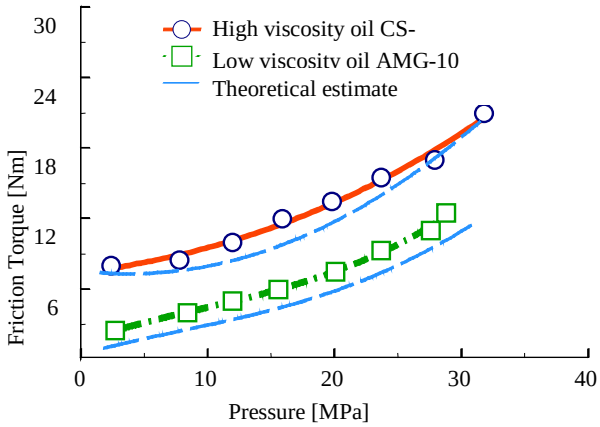

Fig. 5: *The dependence of the friction torque on hydraulic fluid pressure (theoretical calculation and experimental data)*

The friction torque measurement results and theoretical estimation of the total friction torque are illustrated in Fig. 5. Different oil grades were used in this experiment. As shown in Fig. 5, top curve illustrates the BAHM performance on high viscous hydraulic oil CS-46, the bottom one (line and square curve) – on low viscous hydraulic oil AMG-10.

During the friction torque calculation in accordance with Eq. 6, the following data were considered:
R_1 = 10.5 mm ; R_4 = 37.4 mm ; ω = 3000 min^{-1};
Pressure coefficient of viscosity for AMG-10 – is $\alpha = 2.3 \cdot 10^{-4}$ cm^2/N;
Pressure coefficient of viscosity for CS-46 – is $\alpha = 2.8 \cdot 10^{-4}$ cm^2/N.

The calculated VP friction torque at $1.3 \cdot 10^{-3}$ mm gap matches with sufficient accuracy experimentally obtained values.

The above mentioned equations were verified by additional experiments, which were carried out on BAHM, equipped with the hydraulic lifting force control device.

Figure 8 (A-view) shows the VP in original design, and Fig. 8 (B-view) shows the redesigned VP. The external radius of the experimental VP differs from the standard VP external radius. As it follows from Eq. 6, the friction torque is increasing and the experiment data verify this also.

To eliminate influences due to rotational speed, temperature and technological factors that altogether affect viscosity, it is possible to perform the friction torque experiment data in dimensionless form dividing by M_1 (see Fig. 6).

It is necessary to pay attention to some scatter of readings, which is difficult to explain only due to the VP design change. But, it is possible to assert that the cylinder block and VP friction torque depends on the contact surfaces grinding. This fact has a direct connection with the experiment, because during the test, the VP replacement was carried out, without the cylinder block replacement. This fact leads us to the conclusion that within certain limits, the VP is interchangeable.

The hydraulic-mechanical efficiency of the BAHM is defined by the theoretical and the real torque relationship.

$$\eta_{gm} = \frac{M_T - (M_{TF} + \Delta M)}{M_T} \qquad (9)$$

where:

ΔM – torque which is spent on various hydraulic resistances.

$$\Delta M = M_{PF} + M_{SF} + M_{GF} + M_{HF} \qquad (10)$$

In a different BAHM design, besides the main friction torque there is a cardan joint friction torque.

Theoretical research on the BAHM hydraulic-mechanical performance has brought to evidence that a dependence exists on shaft angular speed and working pressure. For example, M_{HF} – depends on BAHM shaft speed only.

For the high flow turbulence, flow friction torque M_{HF} depends on the fluid speed squared.

The BAHM design improvements goal – is to control hydraulic lifting force in the VP gap.

The new overall dimensions of the improved VP, cause a negligible friction torque increase, and low BAHM mechanical performance change, but essentially rise the durability and reliability of the BAHM.

4 Fluid dynamics in VP gap

The definition of the VP gap dependence on various factors is of a great practical interest. Experiments have shown that the normal operating modes of the BAHM provide the fluid film friction in the gap between the VP and rotating cylinder block. Thus, the general hydrodynamic equations are suitable for the hydraulic fluid behavior analysis.

To simplify the calculations, let us assume that the gap height is constant. In this case, the hydraulic fluid dynamics for the parallel VP gap is described by Navier-Stokes equations, which can be solved, to give:

a) radial velocity distribution in the gap:

$$v_r = \frac{1}{2\mu}\cdot\frac{dp}{dr}\cdot\left(y^2 - hy\right) \tag{11}$$

where: y – unit gap.

b) pressure distribution in the gap:

$$p = p_0\frac{\ln\frac{R_4}{r}}{\ln\frac{R_4}{R_3}}\ ;\ R_3 \le r \le R_4$$
$$p = p_0\frac{\ln\frac{r}{R_1}}{\ln\frac{R_2}{R_1}}\ ;\ R_1 \le r \le R_2 \tag{12}$$

c) hydraulic fluid leakages:

$$Q_{OU} = \frac{\pi h^3 p_0}{12\mu\ln\frac{R_4}{R_3}}\ ;\ Q_{IN} = \frac{\pi h^3 p_0}{12\mu\ln\frac{R_2}{R_1}} \tag{13}$$

d) hydraulic lifting force:

$$T_{got} = \pi\cdot p_0\left(\frac{R_4^2 - R_3^2}{\ln\frac{R_4}{R_3}} - \frac{R_2^2 - R_1^2}{\ln\frac{R_2}{R_1}}\right) \tag{14}$$

Also, it is possible to determine the VP friction torque, taking into account the sealing walls sizes between inlet and outlet ports. Eq. 6 after some simplification will be:

$$M_{VF} = \frac{\pi\cdot\omega\cdot\mu}{2h}\left(R_4^4 - R_1^4\right) \tag{15}$$

Thus, the friction torque and the hydraulic fluid leakage can be defined if VP gap height is known.

However, at the given geometrical sizes of the VP, hydraulic fluid viscosity, discharge pressure, it is impossible to obtain the gap height using the main hydrodynamics equation (Navier-Stokes equation).

According to the experiment data, obtained at normal working pressure, it is possible to make a conclusion, that the gap heights are limited between $0.5\cdot10^{-6}$ m and $5\cdot10^{-6}$ m .

The current work relies on the principle of mechanical energy dissipation (Helmholtz principle), in which "the flow is really steady, when the mechanical energy dissipation is minimum" (Happel, 1976). It is supposed, that VP gap and fluid flow provide the minimal rate of the mechanical energy dissipation. In this case the function of function which determine the energy dissipation for different h values, is minimal and equal to:

$$N_{dis} = 2\mu\int_V \dot{S}^2 dv = \int_V \dot{S}_{ij}\dot{S}_{ij}\,dv \tag{16}$$

In cylindrical coordinates, the components of deformation velocity tensor are (Loitsansky, 1973):

$$\dot{S}_{rr} = \frac{\partial v_r}{\partial r};\dot{S}_{yy} = \frac{\partial v_y}{\partial y};$$
$$\dot{S}_{\varphi\varphi} = \frac{1}{r}\cdot\frac{\partial v_\varphi}{\partial\varphi} + \frac{v_r}{r}$$
$$\dot{S}_{ry} = \frac{1}{2}\left(\frac{\partial v_y}{\partial r} + \frac{\partial v_r}{\partial y}\right);$$
$$\dot{S}_{r\varphi} = \frac{1}{2}\left(\frac{1}{r}\cdot\frac{\partial v_r}{\partial\varphi} + \frac{\partial v_\varphi}{\partial r} - \frac{v_\varphi}{r}\right) \tag{17}$$
$$\dot{S}_{\varphi y} = \frac{1}{2}\left(\frac{\partial v_\varphi}{\partial y} + \frac{1}{r}\cdot\frac{\partial v_y}{\partial\varphi}\right);$$
$$\dot{S}_{yr} = \dot{S}_{ry};\dot{S}_{\varphi r} = \dot{S}_{r\varphi}$$

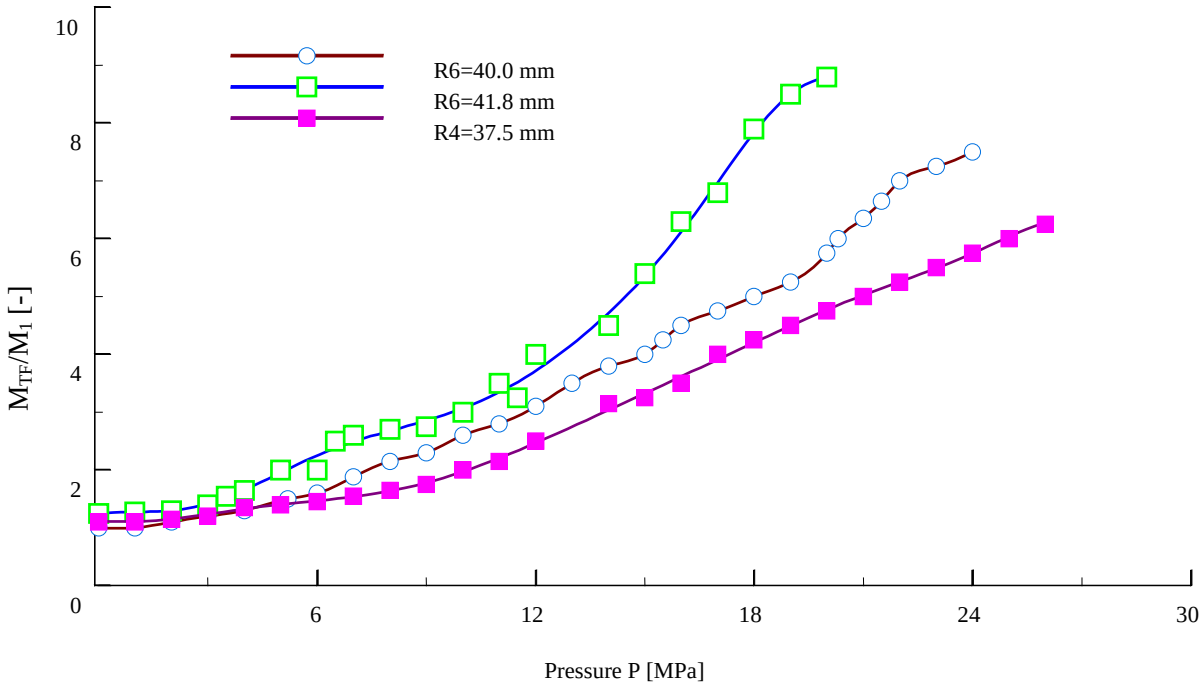

Fig. 6: *Theoretical friction torque at various outward radii*

In the case considered, the peripheral velocity is:

$$v_\varphi = \frac{\omega r y}{h}; (0 \le y \le h) \tag{18}$$

Equation 11 determines the transverse velocity v_y = 0 and radial velocity v_r. If the following flow condition is taken into account:

$$\frac{\partial v_r}{\partial r} << \frac{\partial v_r}{\partial y}; \frac{\partial v_r}{\partial \varphi} = 0; \frac{\partial v_\varphi}{\partial \varphi} = 0$$

the equation of continuity leads us to $\frac{v_r}{r} \sim \frac{\partial v_r}{\partial r}$, then Eq. 16 becomes much simpler:

$$N_{dis} = 2\mu \int_V \left[\begin{array}{l} \frac{1}{2}\left(\frac{\partial v_r}{\partial y}\right)^2 + \frac{1}{2}\left(\frac{\partial v_\varphi}{\partial r} - \frac{\partial v_\varphi}{r}\right)^2 \\ + \frac{1}{2}\left(\frac{\partial v_\varphi}{\partial y}\right)^2 \end{array} \right] dv \tag{19}$$

If we substitute, Eq. 11, 12, 13, 18 in Eq. 19, it transforms to:

$$N_{dis} = \mu \int_0^h dy \cdot \left(\begin{array}{l} \int_{R_1}^{R_2} 2\pi r \cdot \left[\begin{array}{l} \frac{(2y-h)^2}{4\mu^2} \cdot \\ \cdot \left(\frac{dp}{dr}\right)^2 + \\ \frac{\omega^2 r^2}{h^2} \end{array} \right] dr + \\ + \int_{R_3}^{R_4} 2\pi r \cdot \left[\begin{array}{l} \frac{(2y-h)^2}{4\mu^2} \cdot \\ \cdot \left(\frac{dp}{dr}\right)^2 + \\ \frac{\omega^2 r^2}{h^2} \end{array} \right] dr \end{array} \right) =$$

$$= \mu \cdot \left[\begin{array}{l} \frac{\pi p_0^2 h^3}{12\mu^2} \left(\frac{1}{\ln \frac{R_2}{R_1}} + \frac{1}{\ln \frac{R_4}{R_3}} \right) + \\ \frac{\pi \omega^2 \left(R_4^4 - R_3^4 + R_2^4 - R_1^4\right)}{2h} \end{array} \right] \tag{20}$$

Due to the sealing walls between the inlet and outlet VP ports and the rotary movement component, it should be accepted that $R_2 = R_3$ in Eq. 20.

After N_{dis} (h) function test for minimum, we obtain the expression for the gap height, at which the rate of mechanical energy dissipation is minimum.

$$h = \sqrt[4]{\frac{\omega^2 \mu^2}{p_0^2} \cdot \frac{R_4^4 - R_1^4}{\frac{1}{\ln \frac{R_2}{R_1}} + \frac{1}{\ln \frac{R_4}{R_3}}}} \tag{21}$$

Thus, the gap height depends on design of the VP, cylinder block rotation speed, hydraulic fluid viscosity and motor inlet pressure. Equation 21 and 15 prove the obtained friction torque M_{VF} experimental dependencies on motor (Irshov, 1993) inlet pressure p_0 and on hydraulic fluid viscosity factor μ.

However, such factors as: surfaces clearance, fluid structure phenomenon at the distances of $1 \cdot 10^{-6}$ m to the rigid surface, fluid dissipative heating in the VP gap, sophisticated geometry of the VP and other factors, which impair the hydraulic fluid flow were not taken into account in the considered simplified model of the VP gap. These factors may cause the essential deviations of the experimentally obtained VP gap heights in comparison with the estimated values. So, for the actual gap height determination it is necessary to consider the complex gap model, which is based on force balance between outer pressing forces and lifting forces in the gap.

Using Eq. 15 and 21 for the friction torque, we obtain:

$$M_{VF} = \frac{\pi}{2} K \sqrt{\mu \omega p_0} \left[\begin{array}{l} \left(R_4^4 - R_1^4\right)^{\frac{3}{4}} \cdot \\ \cdot \left(\frac{1}{\ln \frac{R_2}{R_1}} + \right. \\ \left. + \frac{1}{\ln \frac{R_4}{R_3}} \right)^{\frac{1}{4}} \end{array} \right] \tag{22}$$

where: K – empirical coefficient.

The comparison of the experimental (see Eq. 22) and calculated friction torque is given in Fig. 7. It was taken into account that the fluid dynamic viscosity depends on pressure p_0, according to the equation:

$$\mu = \mu_0 e^{\alpha \cdot p_0} \tag{23}$$

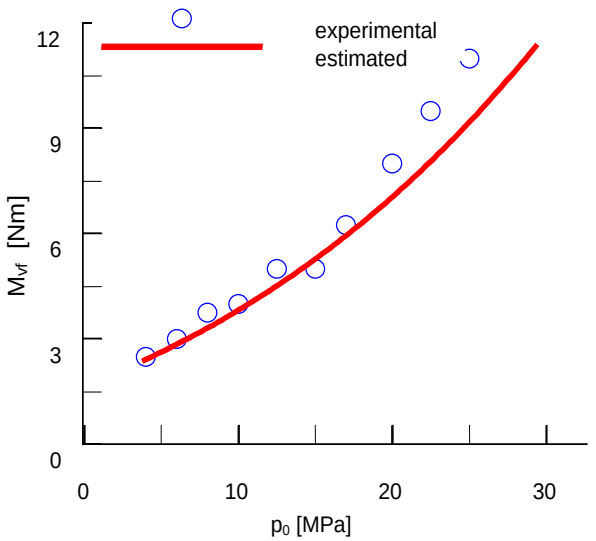

Fig. 7: *The VP gap friction torque (experimental and calculated data)*

As it follows from Fig. 7, Eq. 22 correlates the experimental data well, up to $p_0 \approx 20$ MPa. At higher pressures experimental values grow faster than calcu-

lated data. This phenomenon can be explained as follows: at pressure $p_0 \approx 20$ MPa, the gap height becomes equal to the contact surfaces clearance (see Eq. 15 $h \approx 1 \cdot 10^{-6}$ m), this leads the fluid friction mode change to the mixed boundary-fluid friction mode.

At the $p_0 > 20$ MPa, VP works in a "heavy duty mode", which may cause an excessive heat generation in the VP gap.

5 Traditional VP design calculation

The calculation of the VP was carried out in accordance with the limited pushing and pressing forces ratio on the VP surface. The cylinder block of the tested BAHM was assumed as a rotary part and the VP as a motionless (Gerber, 1970). In non-operational mode, the cylinder block is pressed to the VP by the springs, and in operational mode, the hydraulic pressure provides the additional pressing force. Also there is a hydraulic lifting force in the gap between cylinder block and VP. This force acts in the opposite direction.

Due to the alternation of the cylinder numbers, which are simultaneously connected to the inlet port, the hydraulic pressing force variation is described by a step function.

The average pressing force is equal to:

$$T_{\text{gpr}} = p_0 \frac{\pi d_{\text{p}}^2}{4} \cdot \frac{z}{2} \tag{24}$$

where for the BAHM:
$d_{\text{p}} = 25$ mm; $z = 7$; $T_{\text{gpr}} = 17.17 \cdot 10^{-4} \cdot p_0$ N .

The hydraulic lifting force can be calculated according to the equation, which is deduced with assumption that the pressure diagram on the sealing wall is linear.

$$T_{\text{got}} = p_0 \pi \cdot \left(R_4^2 + R_3^2 - R_2^2 - R_1^2 \right) \tag{25}$$

where for the BAHM:
$R_1 = 10.5$ mm , $R_2 = 16$ mm , $R_3 = 36$ mm,
$R_3 = 32$ mm , $R_4 = 37.5$ mm , $T_{\text{gpr}} = 16.20 \cdot 10^{-4} \cdot p_0$ N

The hydraulic pressing and lifting forces relationship is equal to (spring action was also taken into account):

$$\lambda = \frac{T_{\text{got}}}{T_{\text{gpr}} + T_{\text{spr}}} \tag{26}$$

At low values of inlet pressure, the spring force is commensurate with the hydraulic force while if pressure is increased, the hydraulic force becomes sensibly higher than that due to the spring. It is on this ground that in most practical design calculations, the spring contribution is often neglected.

For the BAHM normal operation in heavy-duty modes, it is important to provide the fluid film in the VP gap in spite of pressing force increase. In this case, the hydraulic lifting force should be equal to the hydraulic pressing force, because the only way to provide the required fluid film thickness in the gap, is to set the equilibrium of lifting and pressing forces (Balkwinsky, 1983). This may be performed through the geometrical features calculation. In this case $\lambda = 1$.

The force balance, according to Eq. 26 without spring force taken into account, is:

$$\lambda \frac{d_{\text{p}}^2}{4} \cdot \frac{z}{2} = R_4^2 + R_3^2 - R_2^2 - R_1^2 \tag{27}$$

The left part in this equation is known but both radii R_4 and R_1 are unknown. As an additional condition for the R_4 and R_1 radii calculation, it is possible to consider the equality of the outflow in the direction of inner and outer sealing walls of the VP. To obtain this condition, it is necessary to equate $\Delta Q_{\text{ou}} = \Delta Q_{\text{in}}$.

The outflows in the VP will be the following:

$$\begin{aligned} \Delta Q_{\text{ou}} &= p_0 \frac{\pi h^3}{12 \mu \ln \dfrac{R_4}{R_3}}; \\ \Delta Q_{\text{in}} &= p_0 \frac{\pi h^3}{12 \mu \ln \dfrac{R_2}{R_1}} \end{aligned} \tag{28}$$

To provide the equality of the outflow in these directions, it is necessary to assume:

$$\ln \frac{R_4}{R_3} = \ln \frac{R_2}{R_1} \tag{29}$$

After these assumptions, we receive the additional equation, which determines the VP geometry:

$$R_4 \cdot R_1 = R_2 \cdot R_3 \tag{30}$$

$$\begin{aligned} R_1^4 + R_1^2 \cdot \left(\lambda \frac{d_{\text{p}}^2}{4} \frac{z}{2} - R_3^2 + R_2^2 \right) - \\ - R_3^2 \cdot R_2^2 = 0 \end{aligned} \tag{31}$$

Without any changes in hydraulic pushing and pressing forces relationship, the VP geometry should be equal: $R_1 = 13.35$ mm and $R_4 = 38.37$ mm. Taking into account that leakages are not equal in all directions, the VP geometry can be adjusted to: $R_1 = 12$ mm, $R_2 = 16$ mm, $R_3 = 32$ mm, $R_4 = 38$ mm. Thus, the factor $\lambda = 0.943$ becomes 0.940.

The leakage flow paths to and from the VP represent a critical issue in durability problems of the BAHM. In fact the solid contaminant, at specific sizes determines excessive wear of the VP surface.

Due to the fact that systems' pressure tends to be increased, the effect on viscosity of both pressure and temperature must be accounted. This fact, at a design stage, will possibly lead to an increase of durability and reliability of the motor.

In an attempt of exerting control over the gap height between the rotating barrel and VP, this last component has been modified in respect to the original design. Two peripheral, yet separated, grooves have been machined on to the VP face (see Fig. 9). These grooves communicate with a throttle device. If this device is close, both grooves filled with fluid contribute in providing additional lifting capacity of the VP with respect to the barrel. By different throttling of fluid out of the grooves, a modulation of the lifting force can be obtained.

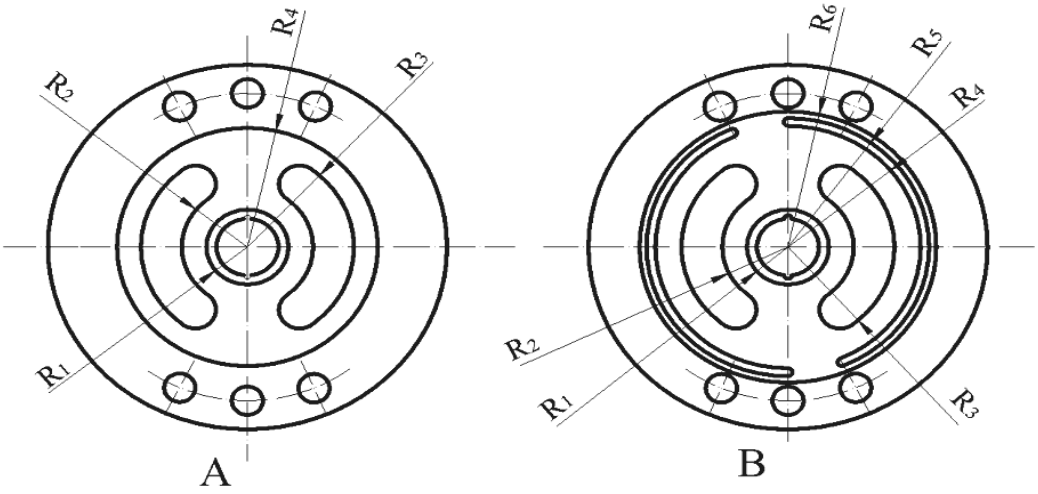

Fig. 8: *The VP of the BAHM (A – traditional design, B – new design)*

6 VP with the hydraulic lifting force control device (HLFCD)

The analytical and experimental investigations of the VP confirm the need for improvements in its design. This paper introduces new VP design that embodies a hydraulic lifting force control device or HLFCD. The improved VP should provide:

- hydraulic lifting force recovery in heavy duty mode operation;
- hydraulic motor output power control due to the leakages regulation in the DPP gap.

The new VP is based on additional hydraulic lifting force action on the VP surface.

Two grooves on the VP front surface (see Fig. 8 and Fig. 9) are filled with the hydraulic fluid due to the radial leakages.

In some cases, when power from the BAHM need to be reduced, it will not be necessary to act on displacement (i.e., decrease the angle between the shaft and barrel). In fact, the throttle valve can possibly provide enough leakage to match the desired reduction of power. The throttling device can be activated by a temperature sensor and may have electric, hydraulic or pneumatic control.

Figure 8(A) shows the standard VP and Fig. 8(B) shows the VP design after improvements application.

This device will solve BAHM reliability problems under all operating conditions, even in presence of pressure peaks or in case of specific applications involving new materials (e.g. composite materials).

The design feature of the HLFCD is the grooves on the front face of the VP, which are not connected to the VP ports (see Fig. 9).

Fig. 9: *The prototype of the VP with the HLFCD*

When the hydraulic pressure is equal to 10…12 MPa, the hydraulic forces relationship variation in the VP is carried out by the throttle valve which blocks the outflow channel tap in the grooves. The backup effect provides the additional pressure and difference of the hydraulic lifting force.

When the hydraulic pressure is over 10…12 MPa, the pressing and lifting forces are larger than the spring force. The forces operational fluctuations do not cause any influence in this case.

The pressing and lifting forces relationship was obtained after the investigation of the BAHM with the HLFCD. In the first test series, pressure in the grooves was consequent to a specific flow rate generated by a separate displacement pump. Starting at a low working pressure in the main pipe, the pressure was increased up to the moment of cylinder block and VP joint seal failure. The results of these measurements are shown in Fig. 11.

According to the diagram, it is possible to establish a correlation between groove pressure p_k and motor inlet pressure p_0.

$$p_k = 0.2\,p_0 + C \tag{32}$$

where: coefficient C = 1.8 MPa.

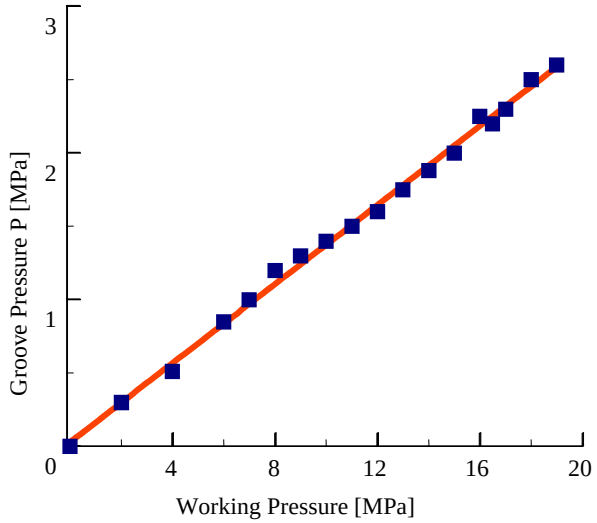

Fig. 10: *Groove pressure dependence on working pressure*

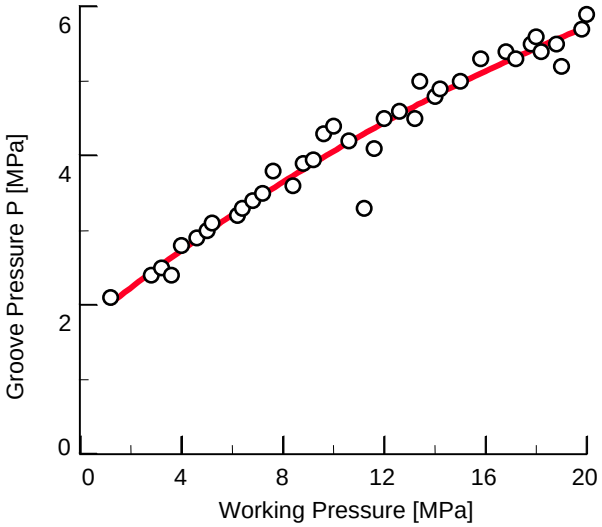

Fig. 11: *Flow in the groove is provided by displacement pump*

Such groove pressure and motor inlet pressure p_0 ratio is typical for the considered BAHM type, and leads to the cylinder block and VP seal failure.

According to Eq. 32, an approximate equation for the hydraulic force will be the following:

$$T'_{\text{got}} = 0.97\frac{\pi}{2}\cdot\begin{bmatrix} 0.5p_0\left(R_2^2-R_1^2\right)+p_0\left(R_3^2-R_2^2\right)+ \\ \left(0.6p_0+\frac{C}{2}\right)\cdot\left(R_4^2-R_3^2\right)+ \\ \left(0.2p_0+C\right)\cdot\left(R_5^2-R_4^2\right)+ \\ \left(0.1p_0+\frac{C}{2}\right)\cdot\left(R_6^2-R_5^2\right) \end{bmatrix} \quad (33)$$

where: T'_{got} – lifting force

The new VP design has a groove width 2.2 mm, and R_5 = 39.7 mm, R_6 = 42 mm.

As it is shown in Fig. 11, the experimental line does not pass through the coordinate origin. Using the experimental results, it is possible to calculate the spring force, in this case, Eq. 34 according to p_0 = 0, is:

$$T_{\text{got}} = T_{\text{spr}} = 0.97\cdot\frac{\pi}{2}\cdot\begin{bmatrix} \frac{C}{2}\left(R_4^2-R_3^2\right)+ \\ C\left(R_5^2-R_4^2\right) \\ +\frac{C}{2}\left(R_6^2-R_5^2\right) \end{bmatrix} \quad (34)$$

The other test series were carried out in conditions, which are close to real operation modes. There was no external pump fluid supply. For the pressure measurement a manometer was used. The working pressure in a groove was rather different from the first test series. This difference is explained by the VP geometry change. By experiment results (see Fig. 10), it is obtained the dependence, which is equal to:

$$p_{\text{k}} = 0.14\,p_0 \quad (35)$$

where: p_{k} – closed groove pressure.

Using the simplified calculating model, it is possible to obtain the theoretical relationship of the pressure in the groove p_{k} and working pressure p_{k}.

$$p_{\text{k}} = 2.9\cdot p_0 \quad (36)$$

In this case, in the real condition hydraulic lifting force is defined by the equation:

$$T_{\text{got}} = \frac{\pi}{2}p_0\cdot\begin{bmatrix} K_1\left(R_2^2-R_1^2\right)+K_2\left(R_3^2-R_2^2\right) \\ +K_3\left(R_4^2-R_3^2\right) \\ +K_4\left(R_5^2-R_4^2\right)+K_5\left(R_6^2-R_5^2\right) \end{bmatrix} \quad (37)$$

For the BAHM is considered:
K_1 = 0.5, K_2 = 1, K_3 = 0.57, K_4 = 0.14, K_5 = 0.7

7 Conclusions

This article presented results of the bent axis hydraulic motor leakages investigation.

Based on the study of the ordinary valve plate, it was revealed that in all bent axis hydraulic motors (including the considered hydraulic unit), the minimum of working fluid leakages in the gap between valve plate and cylinder block is very important for the hydraulic motor normal operation, because it provide the fluid film lubrication and predetermine the reliability and durability level of the hydraulic unit assembly.

The total hydraulic leakages were measured and classified in dependence on their nature. Also it was considered the influence of the different nature friction torques on the mechanical efficiency of the bent axis hydraulic motor. After the carried out investigation, it was introduced the new valve plate design.

With unchanged general geometry sizes, the new VP have shown the ability to recover a hydraulic lifting force in heavy duty mode operation, enabling to create a hydraulic unit which is less sensitive to the hydraulic fluid contaminations, contact surfaces clearance and therefore, more reliable in high pressure and heavy load modes operation.

Although the new BAHM with the hydraulic lifting force control device is not perfect and is to be investigated in deeper detail, it perform better controllability

and reliability than current motors, where the lifting force and gap height is not regulated.

Moreover, the hydraulic lifting force control device enables the opportunity of composite materials application in hydraulic motors.

Nomenclature

$\Delta Q_{1...6}$	leakages	[cm^3/sec]
ΔQ_T	BAHM theoretical capacity	[m^3/sec]
η_V	volumetric efficiency	[–]
Q_m	hydraulic fluid internal leakage	[cm^3/sec]
Q_{out}	hydraulic fluid external leakage	[cm^3/sec]
μ	fluid dynamic viscosity	[P]
p_0	hydraulic fluid pressure	[MPa]
h	gap height	[mm]
$R_{1...2}$	internal and external radii VP inner sealing wall	[mm]
E_V	fluid bulk modulus	[N/m^2]
V	dead zone capacity	[m^3]
M_{VF}	VP friction torque	[Nm]
M_{VB}	bearing friction torque	[Nm]
ω	cylinder block rotational speed	[sec^{-1}]
α	pressure coefficient of viscosity	[cm^2/N]
p	working pressure	[MPa]
$R_{3...4}$	internal and external radii of the VP outer sealing wall	[mm]
z	piston number	[–]
d_p	piston diameter	[mm]
d_{bt}	bearing raceway diameter	[mm]
f	friction coefficient	[-]
M_T	BAHM theoretical torque	[Nm]
M_{TF}	theoretical friction torque	[Nm]
M_{VF}	cylinder block and VP friction torque	[Nm]
M_{BF}	bearings friction torque	[Nm]
M_{PF}	piston and cylinder block friction torque	[Nm]
M_{SF}	piston ball joint friction torque	[Nm]
M_{GF}	lip-type seal friction torque	[Nm]
M_{HF}	flow friction torque	[Nm]
η_{gm}	hydraulic-mechanical efficiency	[-]
M_1	unit moment	[Nm]
T_{got}	hydraulic lifting force	[N]
T_{gpr}	hydraulic pressure force	[N]
T_{spr}	spring force	[N]
N_{dis}	energy dissipation velocity	[-]
$\dot{S}_{rr}$, $\dot{S}_{r\varphi}$	strain rate tensor components	[-]
v_φ	peripheral velocity	[m/sec]
v_y	transverse velocity	[m/sec]
v_r	radial velocity	[m/sec]
λ	forces ratio factor	[-]
p_k	closed groove pressure	[MPa]
$K_{1...5}$	pressure ratio empirical coefficients	[-]

References

Balkwinsky, J. 1983. *Hydraulic motors.* Elmonds & Sons Press Ltd.

Bashta, T. M. 1974. *Displacement pumps and hydraulic motors.* USSR, Moscow. Mashinostroenie Publishing.

Gerber, H. 1970. Rudiments of calculation for axially acting pistons and flat lapped distributor volumetric machines. *Hydraulic & Pneumatic Power*. Vol. 16, No 188, pp. 470 – 482.

Happel, J. and **Brenner, G.** 1976 *Hydrodynamics at small Reynolds numbers.* USSR, Moscow. Mir Publishing Corporation.

Irshov, B. I. and **Karasaevich, G. F.** 1993. Investigating the bent axis hydraulic motors valve plate gap. *Westnik Mashinostroenie.* Vol. 1, pp. 22 – 27.

Khrapak, A. V. 2000. Axial piston hydraulic motors design features analysis. *Refrigeration engineering and technology.* Vol. 67, pp. 5 – 7.

Loitsansky, L. 1973 *Fluid mechanics*. Moscow. Nauka Publishing Corporation.

Minchevich, V. A. 1983. Fluid dynamics in axial piston hydraulic motors, *Friction and excessive wear.* Vol. 4, pp. 728 – 732.

Murashko, V. P., Bochkovaya, L. F. and **Khrapak, A.V.** 1999. The equation of the axial piston hydraulic motor cylinder block rotation, *Annual Proceedings of the Odessa State Polytechnic University.* Vol. 3, pp. 68 – 71.

Paulis, R. 1991 *Lubrications in hydraulic motors*. Urmas Print. Riga. Latvia.

Alex V. Khrapak
Born in 1977 in Odessa (Ukraine). Graduated from Odessa State Polytechnic University, gained MSc degree in Mechanical Engineering. During study, was active in rigid body research works. From 1998 till 2000 scientific employee at OSPU. Since October 1999 PhD student at Odessa State Academy of Refrigeration. Since January 2000, co-operated with "Stroyhydraulika" (hydraulic motors plant) in the field of motors design improvements.